Dalton Transactions

PAPER

View Article Online
View Journal | View Issue

Cite this: *Dalton Trans.*, 2015, **44**, 10304

2-(2′-Pyridyl)-4,6-diphenylphosphinine *versus* 2-(2′-pyridyl)-4,6-diphenylpyridine: synthesis and characterization of novel Cr^0, Mo^0 and W^0 carbonyl complexes containing chelating P,N and N,N ligands†

Iris de Krom,[a] Martin Lutz[b] and Christian Müller*[a,c]

Received 1st April 2015,
Accepted 7th May 2015

DOI: 10.1039/c5dt01261a

www.rsc.org/dalton

Replacing nitrogen by phosphorus in otherwise similar structures changes the properties of the resulting compounds significantly due to the electronic differences that exist between these heteroatoms. While the "hard" nitrogen atom of the pyridine moiety acts as a good σ-donor, the "soft" phosphorus atom of the phosphinine core results in a rather strong π-acceptor capacity. A series of novel group 6 complexes $[M(CO)_4(L\text{^}L)]$ (M = Cr^0, Mo^0, W^0) have been synthesized, in which L^L is either 2-(2′-pyridyl)-4,6-diphenylphosphinine (P,N) or the corresponding bipyridine derivative, 2-(2′-pyridyl)-4,6-diphenylpyridine (N,N) as a chelating, bidentate ligand. The here presented results describe a detailed investigation of the structural and spectroscopic properties of the coordination compounds $[M(CO)_4(P,N)]$ and $[M(CO)_4(N,N)]$ (M = Cr^0, Mo^0, W^0), leading to a better understanding of such intriguing aromatic phosphorus heterocycles.

Introduction

α-Diimines (–N=C–C=N–), such as 2,2′-bipyridine (bpy) (Fig. 1), are well studied nitrogen ligands. Their rich coordination chemistry has often been exploited for the development of molecular devices and homogeneous catalytic systems because of their versatile spectroscopic, photochemical and electrochemical properties.[1–11] Tetracarbonyl-(α-diimine) complexes $[M(CO)_4(\alpha\text{-diimine})]$ of group 6 transition metals (M = Cr^0, Mo^0, W^0) are interesting because of the unique combination of an electron-rich, low valent metal atom, stabilized by four CO ligands, and an electron accepting α-diimine ligand.[12–20] These compounds usually have low-lying metal-to-ligand (MLCT) charge-transfer excited states and thus play an important role for understanding the spectroscopic, photophysical and photochemical behavior of such chromophores.

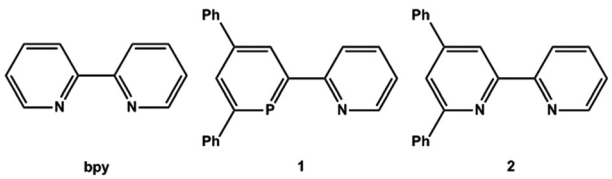

Fig. 1 α-Diimine 2,2′-bipyridine (bpy), pyridyl functionalized phosphinine **1** and its bipyridine derivative **2**.

In fact, the lowest lying MLCT state is responsible for several remarkable features, such as a negative solvatochromism and an interesting luminescence in solution.

The replacement of a pyridine unit in bpy by a π-accepting λ^3-phosphinine entity leads to 2-(2′-pyridyl)-4,6-diphenylphosphinine (**1**) (Fig. 1), a semi-equivalent of bipyridine containing a low-coordinate "soft" phosphorus and a "hard" nitrogen heteroatom.[21–30] Such chelates are intriguing bidentate P,N hybrid ligands, which have recently been explored extensively by our group.[28,31–35]

Substituting nitrogen by phosphorus in similar structures causes rather diverse properties of the resulting compounds due to the electronic difference that exists between these heteroatoms.[23–28,34–39] As a matter of fact, the electronic properties of phosphinines differ substantially from those of pyridines, as shown by photoelectron and electron transmission spectroscopy as well as by theoretical calculations.[40] The

[a]*Schuit Institute of Catalysis, Department of Chemical Engineering and Chemistry, Eindhoven University of Technology, 5600 MB Eindhoven, The Netherlands*
[b]*Bijvoet Center for Biomolecular Research, Department of Crystal and Structural Chemistry, Utrecht University, 3584 CH Utrecht, The Netherlands*
[c]*Institut für Chemie und Biochemie, Freie Universität Berlin, Fabeckstr. 34-36, 14195 Berlin, Germany. E-mail: c.mueller@fu-berlin.de*

†Electronic supplementary information (ESI) available: Experimental procedure for the preparation and electrochemical characterization of all coordination compounds as well as X-ray crystallographic information. CCDC 1056137–1056141. For ESI and crystallographic data in CIF or other electronic format see DOI: 10.1039/c5dt01261a

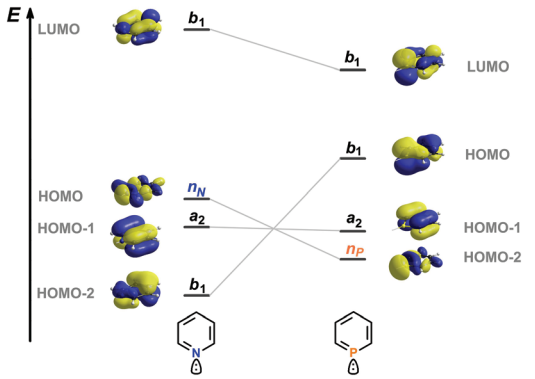

Fig. 2 Frontier orbitals of C_5H_5N and C_5H_5P.

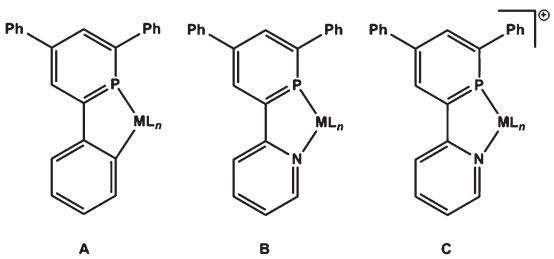

Fig. 3 Coordination compounds **A**–**C** containing phosphinine ligands.

HOMO−2 has a large coefficient at the phosphorus atom, and essentially represents the lone pair at the heteroatom (Fig. 2).

The phosphorus lone pair occupies a more diffuse and less directional orbital than that of pyridine. While the HOMO−1 and HOMO contribute to π-donation, the LUMO, with a large coefficient at the phosphorus atom, enables the heterocycle to act as a π-acceptor ligand, once coordinated to the metal center *via* the phosphorus atom. Consequently and in contrast to pyridines, phosphinine-based ligands are especially suitable for the stabilization of electron-rich metal centers due to their pronounced π-acceptor properties.[28] As expected, the electronic properties of the chelating P,N hybrid ligand **1** easily allows the synthesis of $[M^1L_n(\mathbf{1})]$ complexes by reaction of **1** with $[Rh(cod)_2]BF_4$ (cod = 1,5-cyclooctadiene) or $[Re(CO)_5Br]$ and both compounds were characterized crystallographically.[27,32] More importantly, also the rather challenging preparation of phosphinine-based complexes with metal centers in medium oxidation states has been achieved recently by our group for the first time. The hitherto unknown cyclometalated compounds of type **A** as well as M^{II} and cationic M^{III} complexes of type **B** and **C** (Fig. 3), respectively, were also characterized crystallographically.[28,31,32,41–43]

Interestingly, the strategy used for the synthesis of phosphinines *via* the pyrylium salt route, originally reported by Märkl, also allows the preparation of the bipyridine derivative 2-(2′-pyridyl)-4,6-diphenylpyridine (**2**, Fig. 1). This compound has an identical substitution pattern as **1**, which consequently makes a direct comparison of the chelating ligands as well as their corresponding transition metal complexes possible.[27,28,32,42]

Here we report on the synthesis and characterization of a series of the group 6 complexes $[M(CO)_4(L\hat{}L)]$ (M = Cr^0, Mo^0, W^0), in which L^L is 2-(2′-pyridyl)-4,6-diphenylphosphinine (**1**) or the corresponding bipyridine derivative, 2-(2′-pyridyl)-4,6-diphenylpyridine (**2**). A detailed comparison of the structural and spectroscopic data will be presented, which allows an evaluation caused by the different heteroatoms in otherwise identical compounds.

Results and discussion

Synthesis of coordination compounds

Hexacarbonyl complexes of Cr^0, Mo^0 and W^0 are kinetically rather stable, making thermal ligand substitution reactions sometimes difficult and unselective. We therefore attempted the synthesis of the carbonyl complexes of **1** and **2** both under photochemical and thermal reaction conditions. It turned out, that the 18 VE Cr^0 complexes **3** and **6** (Scheme 1) can easily be obtained quantitatively by reacting $[Cr(CO)_6]$ with ligand **1** or **2** under irradiation with UV-light in THF for 8 and 24 hours, respectively. We also observed that **3** and **6** are accessible in rather good yields under thermal reaction conditions. The reaction towards the Cr^0 complex **3** was monitored by means of $^{31}P\{^1H\}$ NMR spectroscopy and the course of the ligand substitution under UV-light is depicted in Fig. 4 (top). Coordination compound **3** shows a characteristic downfield shift of the phosphorus resonance in the $^{31}P\{^1H\}$ NMR spectrum at δ (ppm) = 246.0 (**3**), in contrast to phosphinine-based transition metal complexes of Rh(I), Pd(II), Pt(II), Rh(III) and Ir(III), in which the phosphorus signal is shifted upfield from the one of the free ligand (δ (ppm) = 189.0 (**1**)).[44–46]

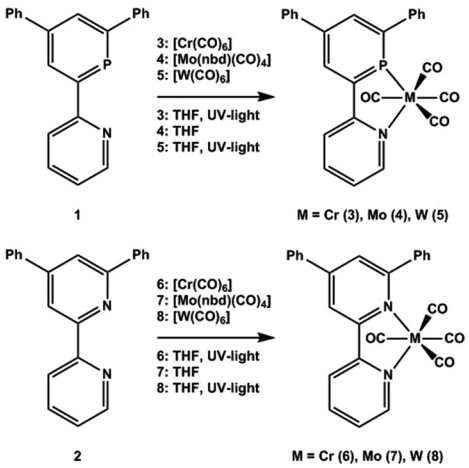

Scheme 1 Synthesis of tetracarbonyl complexes **3**–**8** containing **1** and **2**.

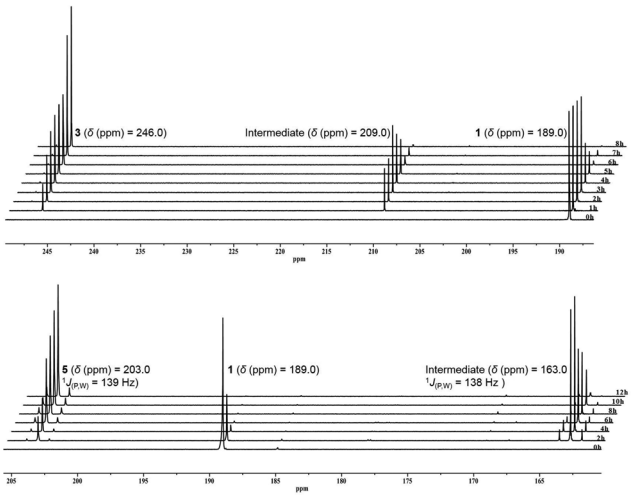

Fig. 4 Time-dependent $^{31}P\{^1H\}$ NMR spectra for the conversion of **1** with $[Cr(CO)_6]$ (top) and $[W(CO)_6]$ (bottom) towards **3** and **5**, respectively.

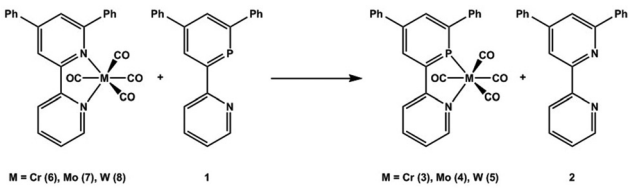

Scheme 2 Ligand exchange of bipyridine **2** from complexes **6–8** with the P,N ligand **1** under formation of coordination compounds **3–5**.

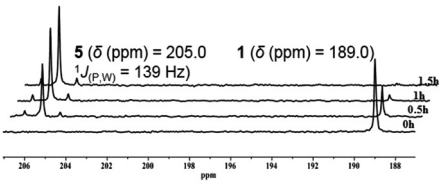

Fig. 5 Time-dependent $^{31}P\{^1H\}$ NMR spectra for the ligand exchange of the bipyridine derivative **2** by the P,N hybrid ligand **1** under formation of complex **5** in toluene at T = 120 °C.

Interestingly, an intermediate is observed upon consumption of the ligand at δ (ppm) = 209.0. We attribute this resonance to the formation of the mono-substituted complex $[W(CO)_5(N,\eta^1\text{-}P)]$, in which only one carbonyl ligand has been replaced by the phosphorus-containing heterocycle, prior to the formation of the final product **3**. Similar behavior has been observed by Mathey *et al.* for the reaction of 2-(2′-pyridyl)-4,5-dimethylphosphinine (NIPHOS) with $[Cr(CO)_6]$.[44] Because of the presence of a "soft" phosphinine and a "hard" pyridine donor, which would certainly react in a different manner, it is anticipated that the coordination of the P,N hybrid ligand will take place in two steps starting with coordination of the phosphorus donor to the metal center, followed by formation of the chelate through coordination of the nitrogen atom.

The phosphinine-complex $[Cr(CO)_5L]$ has been reported in literature by Nöth *et al.* and a chemical shift difference of $\Delta\delta$ (ppm) = 18.0 has been observed for the signals of 2,4,6-triphenylphosphinine and the complex by means of $^{31}P\{^1H\}$ NMR spectroscopy.[44] This value is in the same range observed for **1** and the intermediate at δ (ppm) = 209.0 ($\Delta\delta$ (ppm) = 20.0). Apparently, this species can be observed only during the photochemical ligand substitution reaction, as we could not observe this intermediate while performing the reaction thermally.

The complexes based on molybdenum (**4** and **7**, Scheme 1) could easily be synthesized starting from commercially available $[Mo(nbd)(CO)_4]$ (nbd = norbornadiene) and one equivalent of **1** or **2**. The ligand substitution reactions were completed at room temperature within 1 and 3 hours, respectively. The W^0 complexes **5** and **4** (Scheme 1) were obtained by mixing $[W(CO)_6]$ with ligand **1** and **2**, respectively, in toluene and heating the reaction mixture at T = 120 °C. It turned out, that only 60 to 70% of the starting material was converted to the final compound after 48 hours. However, irradiation of a THF solution of $[W(CO)_6]$ and ligand **1** or **2** with UV-light for 12 and 48 hours, respectively, led to full conversion of the starting material. When following the course of the ligand substitution reaction by means of $^{31}P\{^1H\}$ NMR spectroscopy, (Fig. 4 bottom) an intermediate is again observed at δ (ppm) = 163.0 ($^1J_{(P,W)}$ = 138.0 Hz). Interestingly, the coupling between the tungsten and phosphorus nuclei shows indeed that first the phosphorus donor is coordinated to the W^0 center, followed by coordination of the nitrogen atom under formation of **5**.

We were further interested in a competition experiment between the P,N hybrid ligand **1** and the N,N analogue **2** with respect to their coordination capacity to a rather electron-rich transition metal center. We thus reacted one equivalent of **1** with the coordination compounds **6**, **7** and **8**. It turned out that the bipyridine derivative **2** was almost quantitatively replaced by phosphinine **1** under formation of the corresponding $[M(CO)_4(L\hat{}L)]$ complexes (M = Cr, Mo, W) within a few hours (Scheme 2).

In the case of the tungsten complex **8**, the ligand exchange reaction under formation of **5** by refluxing in toluene proceeds almost quantitatively within 3 hours. This reaction can easily be followed by means of $^{31}P\{^1H\}$ NMR spectroscopy, as depicted in Fig. 5 for the conversion of **8** into **5**.

As anticipated before, the P,N-hybrid ligand **1** is a much better π-acceptor and thus prefers coordination to a low-valent metal center in contrast to the bipyridine derivative **2**. Mathey *et al.* already described a similar competition experiment, in which 2,2′-bipyridine was displaced by NIPHOS from an electron rich Ir^I and Rh^I fragment.[47] For the molybdenum analog the reaction already takes place at room temperature in DCM. However, in order to convert complex **7** into coordination compound **4**, a reaction time of 72 hours was needed. The displacement of **2** from the corresponding chromium complex was, on

the other hand, completed within 3 hours in refluxing DCM. This reaction does not take place at room temperature. This was also observed for the tungsten complex, which formation also requires higher reaction temperatures.

Crystallographic characterization

Crystals of the coordination compounds **4–8** suitable for X-ray diffraction could be obtained. The orange phosphinine-based complexes **4** and **5** are isomorphous in the acentric orthorhombic space group $Pna2_1$, while the red bipyridine-based coordination compounds **6** and **7** are isomorphous in the centrosymmetric triclinic space group $P\bar{1}$ (no. 2). Compound **8** crystallizes in the centrosymmetric monoclinic space group $P2_1/c$. The molecular structures are depicted in Fig. 6 and 7, along with selected bond lengths and angles listed in Tables 1 and 2, respectively.

The X-ray crystal structure analyses confirm the mononuclear nature of the coordination compounds with ligand **1** and **2** acting as a bidentate chelate. As known from many structurally characterized complexes of the type $[M(CO)_4(N\hat{}N)]$ (M = Cr, Mo, W), the axial carbonyls in **4–8** bend away from the chelating P,N and N,N ligand as a result of minimizing the electron repulsion between the relevant orbitals for σ-donation and π-back donation, which are involved in the complex formation. This is exemplarily shown by the side views of the complexes $[Mo(CO)_4(P,N)]$ (**4**) and $[Mo(CO)_4(N,N)]$ (**7**) in Fig. 8a and c, respectively, in which the two additional phenyl groups are omitted for clarity and only the *ipso*-carbon atoms are shown. Unfortunately, it is not possible to correlate in this particular case the C_{ax}–M–C_{ax} angle with the electron withdrawing character of the bidentate ligand because two different heteroatoms are present in **4**, which should have an influence on the coordination geometry. From the same graphical representation it is further obvious, that the two heterocyclic rings in all compounds are not perfectly coplanar with respect to one another. Nevertheless, in contrast to coordination compounds **4** and **5**, the molecular structure of the bipyridine-based complexes **6–8** reveal a strong distortion, as the two pyridine rings are notably twisted (torsion angle N(1)–C(5)–C(6)–N(2) = −13.22(15)° (**6**), −13.95(16)° (**7**), −18.4(2)° (**8**), with interplanar angles between the least-square planes = 15.52(6)° (**6**), 16.03(6)° (**7**), 23.18(8)° (**8**)). The distortion is about the same for the isostructural **6** and **7**, however, more pronounced for **8**. This effect might be due to the fact that the phenyl-group in α-position of the phosphorus and nitrogen-heterocycle leads to a repulsive interaction with the $M(CO)_4$ fragment, causing ultimately a distortion of the ligand as well. The intercyclic C(5)–C(6) bond lengths are with 1.476(3) Å (**4**), 1.476(4) Å (**5**), 1.4762(16) Å (**6**), 1.4825(17) Å (**7**), and 1.469(2) Å (**8**) are all very similar.

A comparison of the molecular structures of the P,N-based complexes and N,N-derivatives nicely shows the difference between the aromatic pyridine and phosphinine rings. This is

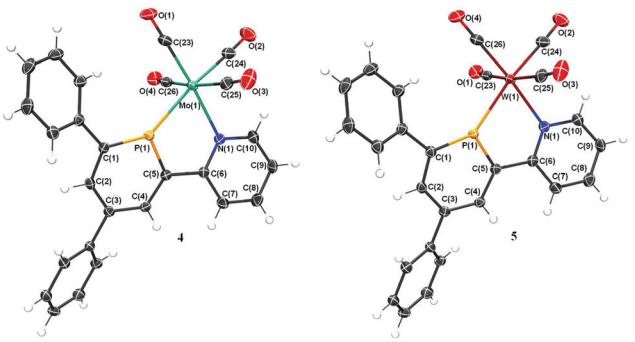

Fig. 6 Molecular structure of phosphinine-based coordination compounds **4** and **5** in the crystal. Displacement ellipsoids are shown at the 50% probability level.

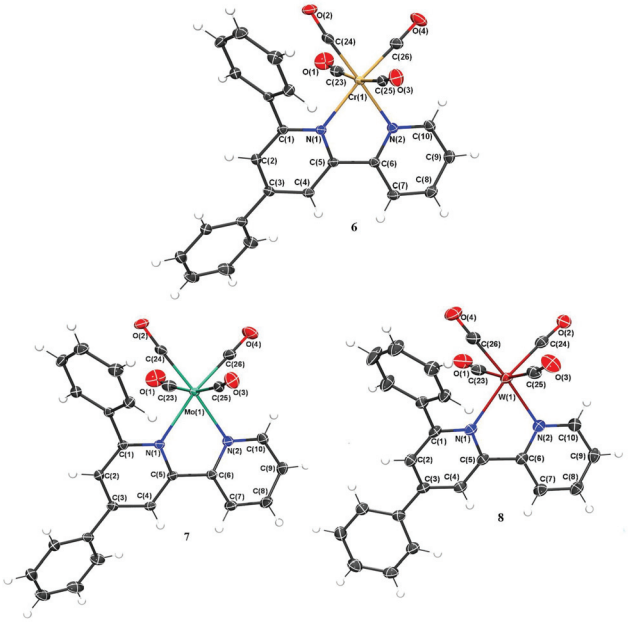

Fig. 7 Molecular structure of bipyridine-based coordination compounds **6–8** in the crystal. Displacement ellipsoids are shown at the 50% probability level.

Table 1 Selected bond lengths (Å) and angles (°) for phosphinine-based coordination compounds **4** and **5**

Bond	**4** (Mo)	**5** (W)
M(1)–P(1)	2.4790(5)	2.4660(6)
M(1)–N(1)	2.303(2)	2.291(2)
C(5)–C(6)	1.476(3)	1.476(4)
P(1)–C(1)	1.737(2)	1.725(3)
P(1)–C(5)	1.733(2)	1.728(3)
C(1)–C(2)	1.394(3)	1.402(3)
C(2)–C(3)	1.396(3)	1.397(3)
C(3)–C(4)	1.399(3)	1.395(4)
C(4)–C(5)	1.393(3)	1.394(4)
N(1)–C(6)	1.363(3)	1.358(3)
N(1)–C(10)	1.345(3)	1.350(4)
C(1)–P(1)–C(5)	104.34(10)	104.84(12)
P(1)–M(1)–N(1)	74.21(5)	74.23(6)

Table 2 Selected bond lengths (Å) and angles (°) for phosphinine-based coordination compounds **6–8**

Bond	**6** (Cr)	7 (Mo)	**8** (W)
M(1)–N(1)	2.1566(10)	2.2929(10)	2.2932(13)
M(1)–N(2)	2.1037(10)	2.2405(11)	2.2312(13)
C(5)–C(6)	1.4762(16)	1.4825(17)	1.469(2)
N(1)–C(1)	1.3550(15)	1.3553(16)	1.360(2)
N(1)–C(5)	1.3601(15)	1.3596(16)	1.3645(19)
C(1)–C(2)	1.3910(17)	1.3926(27)	1.392(2)
C(2)–C(3)	1.3945(17)	1.3944(18)	1.400(2)
C(3)–C(4)	1.3971(17)	1.3964(18)	1.394(2)
C(4)–C(5)	1.3898(17)	1.3896(18)	1.383(2)
N(2)–C(6)	1.3530(15)	1.3522(16)	1.354(2)
N(2)–C(10)	1.3466(16)	1.3470(17)	1.348(2)
C(1)–N(1)–C(5)	117.07(10)	117.43(11)	116.77(13)
N(1)–M(1)–N(2)	76.20(4)	72.30(4)	72.71(5)

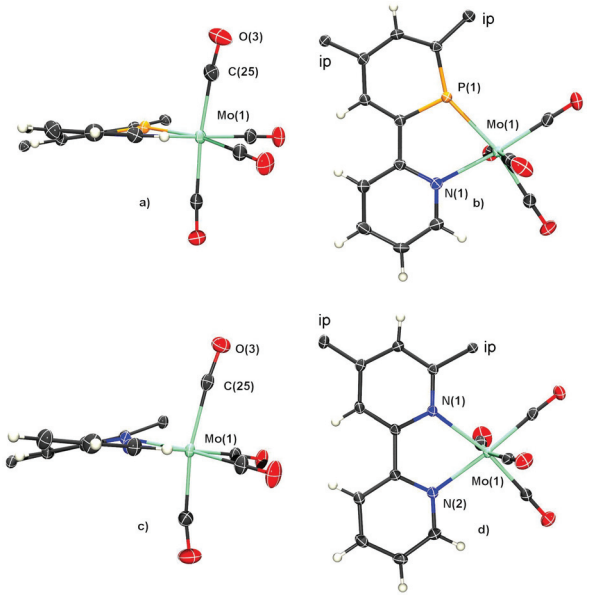

Fig. 8 Molecular structures of the Mo^0 complexes **4** and **7** in the crystal. Displacement ellipsoids are shown at the 50% probability level. (a, c): side view. (b, d): top view. The two additional phenyl groups are omitted for clarity and only the *ipso*-carbon atoms (ip) are shown.

especially obvious from the graphical representation of the molybdenum complexes **5** and **8** in Fig. 8b/d.

Due to the larger P–C bond length in comparison to an N–C bond length, the phosphorus heterocycle is not a regular hexagon but distorted with C–P–C angles of 104.34(10)° (**4**) and 104.84(12)° (**5**), in contrast to the nearly 120° found for the C–N–C angles in the pyridine moieties. The P(1)–C(5) bonds are 1.733(2) Å (**4**) and 1.728(3) Å (**5**), which is very similar to the corresponding bond in the [RhCl(Cp*)(**1**)]Cl and [IrCl(Cp*)(**1**)]Cl complexes of type **C** (Fig. 2) (1.720(2) Å and 1.710(6) Å, respectively).[31] Moreover, the P(1)–C(1) and P(1)–C(5) bond lengths of 1.737(2)/1.733(2) Å (**4**) and 1.725(3)/1.728(3) Å (**5**) are somewhat shorter than in a free triarylphosphinine (1.74–1.76 Å),[48] whereas the C–C bond lengths in the aromatic phosphinine subunit are in the usual range (1.393(3)–1.399(3) Å in **4** and 1.394(4)–1.402(3) Å in **5**) observed for both free and coordinated phosphinine ligands. As expected, the M(1)–N(2) distance in **6** (2.1037(10) Å) is much smaller than in **7** (2.2405(11) Å) and in **8** (2.2312(13) Å). Consequently, the bite angles N(1)–M(1)–N(2) are very similar for **7** (72.30(4)°) and **8** (72.71(5)°), while the bite angle in **6** is much larger (76.20(4)°). The M(1)–N bond lengths in **6–8** are shorter compared to the corresponding M(1)–N(2) bonds in the coordination compound **4** and **5**, due to the presence of a phosphorus atom, rather than a nitrogen atom. As a result, the bite angles P(1)–M(1)–N(1) in the phosphinine-based complexes are with 74.21(5)° (**4**) and 74.23(6)° (**5**) larger than the N(1)–M(1)–N(2) bite angles in **7** and **8**.

As observed before, the metal centers are not located in the ideal axis of the phosphorus lone pair but clearly shifted towards the nitrogen atom. This is especially obvious from the graphical representation of the molybdenum complexes **4** and **5** in Fig. 8b/d. We observed values of C(1)–P(1)–Mo(1) = 147.12(8)°, C(5)–P(1)–Mo(1) = 106.47(7)°, C(1)–P(1)–W(1) = 146.71(10)°, C(5)–P(1)–W(1) = 106.80(9)°. Clearly, this effect is necessary for an efficient complexation of the metal atom by the chelating P,N ligand and facilitated by the more diffuse and less directional lone pair of the low-coordinate phosphorus atom relative to the sp^2-hybridized nitrogen atom in pyridines. Consequently, this is not observed for the M(1)–N(1) interaction in **4** and **5**, for which values of C(6)–N(1)–Mo(1) = 124.51(14)°, C(10)–N(1)–Mo(1) = 118.08(16)°, C(6)–N(1)–W(1) = 124.62(17)°, C(10)–N(1)–W(1) = 117.85(18)° were found. Moreover, the phenyl substituents in the α-position of the phosphorus heterocycle are shifted away from the coordination site and are additionally rotated out of the plane of the phosphorus heterocycle (torsion angles P(1)–C(1)–C(11)–C(12) = 36.4(3)° (**4**) and 36.0(4)° (**5**)).[49] As already pointed out by Le Floch *et al.* the C(1)–P(1)–C(5) angle of the coordination compounds gives an indication of the reactivity of the P=C double bond, especially towards nucleophilic attack. Upon coordination of the lone pair of the phosphorus atom with a high *s* character in the free ligand, it must gain considerable in *p* character. This leads to an opening of the internal C(1)–P(1)–C(5) angle, which is approximately 100° in a free phosphinine. Because this phenomenon can be correlated with the electron-accepting character of a metal fragment, it appears interesting to compare the C(1)–P(1)–C(5) angle in **4** and **5** with selected literature data. For the cationic complexes [RhCl(Cp*(**1**)]Cl and [IrCl(Cp*)(**1**)]Cl the values are 106.64(12)° and 106.7(3)°, respectively. The large opening of this C(1)–P(1)–C(5) angle reflects significant disruption of the aromaticity and consequently leads to a high reactivity of the P=C double bond towards nucleophilic attack.[31] This has indeed been observed experimentally, as these complexes react immediately with water or alcohols at the P=C double bond. In the Cr^0 complex $[Cr(CO)_4(tmbp)]$ (tmbp = tetramethylbisphosphinine), the C(1)–P(1)–C(5) angle is with 104.3° significantly smaller. Interestingly, this compound is highly stable towards nucleophilic attack.[50] For compounds **4** and **5**, we find values of 104.34(10)°

Table 3 IR-wavenumbers $\tilde{\nu}_{(CO)}$ of **3–8**

	$\tilde{\nu}_{(CO)}$ (cm)$^{-1}$
[Cr(CO)$_4$(**1**)] (**3**)	2011; 1910; 1870
[Mo(CO)$_4$(**1**)] (**4**)	2018; 1914; 1869
[W(CO)$_4$(**1**)] (**5**)	2008; 1893; 1870; 1836
[Cr(CO)$_4$(**2**)] (**6**)	2003; 1886; 1859; 1812
[Mo(CO)$_4$(**2**)] (7)	2002; 1898; 1865; 1813
[W(CO)$_4$(**2**)] (**8**)	1995; 1873; 1849; 1810

and 104.84(12)°, respectively. The opening is similar to [Cr(CO)$_4$(tmbp)] and indeed both compounds are also highly stable towards nucleophilic attack as a reaction with water or methanol cannot be observed even at elevated temperatures.

The CO ligands in the coordination compounds are ideal IR-probes to evaluate and to compare the electronic properties of the P,N and the N,N ligands. We thus further investigated coordination compounds **3–8** by means of IR-spectroscopy. In agreement with related 18 VE carbonyl compounds, all complexes show the characteristic wavenumbers $\tilde{\nu}_{(CO)}$ centered around 1900 cm^{-1} (Table 3).

Within one series of the group 6 metal complexes, the values of the IR stretching frequencies vary only marginally. However, it is obvious that the coordination compounds containing the P,N-hybrid ligand (**3–5**) show significantly higher CO stretching frequencies than the bipyridine based coordination compounds (**6–8**). As anticipated, this phenomenon can be attributed to the higher π-accepting character of the phosphinine heterocycle compared to the more σ-donating pyridine moiety.

Solvatochromism

The absorption spectra of the complexes were studied in different organic solvents. Coordination compounds **3–8** exhibit two or three bands in the region between λ = 350–600 nm (Fig. 9). Table 4 lists the spectral data for complexes **3–8** recorded in DCM at room temperature. In analogy to known [M(CO$_4$)L$_2$] complexes these bands can be assigned to MLCT transitions d(M^0) → π*(ligand), as these bands are absent in the free ligands.

Because low-lying MLCT states are usually responsible for several features, such as negative solvatochromism, we were further interested in the absorption spectra of coordination compounds **3–8** in different solvents. In fact, MLCT transitions can be susceptible to solvent polarity and exhibit a blue shift of the MLCT maxima with increasing solvent polarity (negative solvatochromism).[15,17,51–53] We therefore investigated the absorption spectra of the complexes in toluene, tetrahydrofurane (THF), dichloromethane (DCM), dimethylformamide (DMF) and dimethylsulfoxide (DMSO) and the results are depicted in Fig. 10 and 11, respectively, as well as Table 5.

We first focused on the phosphinine-based coordination compounds **3–5**. Unfortunately, complex **3** could not be measured in toluene because of its low solubility in this solvent. However, we observed a blue shift of $\Delta\lambda$ = 11 and

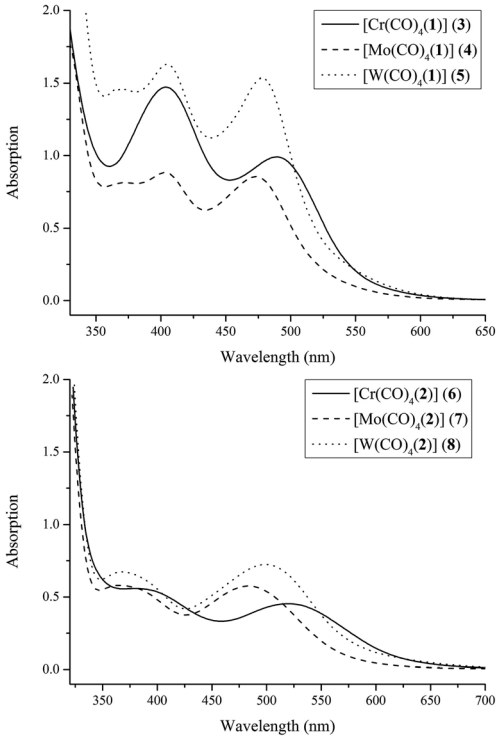

Fig. 9 Absorption spectra of complexes **3–8** (1.25 × 10^{-4} M DCM solutions at T = 298 K).

Table 4 Absorption spectral data of complexes **3–8**

	λ_{max}/nm (10^{-3} ε/M^{-1} cm^{-1})[a]
[Cr(CO)$_4$(**1**)] (**3**)	498 (7.618); 404 (11.330)
[Mo(CO)$_4$(**1**)] (**4**)	473 (6.577); 403 (6.791); 372 (6.392)
[W(CO)$_4$(**1**)] (**5**)	478 (11.806); 404 (12.521); 370 (11.229)
[Cr(CO)$_4$(**2**)] (**6**)	520 (3.486); 379 (4.296)
[Mo(CO)$_4$(**2**)] (7)	483 (4.436); 364 (4.463)
[W(CO)$_4$(**2**)] (**8**)	498 (5.569); 386 (5.173)

[a] 1.25 × 10^{-4} M in DCM at T = 298 K.

16 nm for the two MLCT bands in going from THF to the highly polar DMSO solvent. The molybdenum and tungsten complexes (**4** and **5**) were soluble in all solvents. In this case we noticed a clear shift of the two MLCT bands of $\Delta\lambda$ = 24 and 11 nm for **4**, and $\Delta\lambda$ = 25 and 35 nm for **5** in going from the non-polar to the polar solvent. Both the Mo und W complex show a third band in the high-energy region around λ = 360 nm, which is apparently not affected by the solvent polarity, as this band hardly shifts upon changing the solvent.

The bipyridine-based complexes **6–8** show a prominent MLCT band at around λ = 550 nm. The second band in the high-energy region hardly shifts upon changing the solvent, as observed for the phosphinine-based complexes. We noticed a strong blue shift of the MLCT bands of $\Delta\lambda$ = 64 (**6**), $\Delta\lambda$ = 56 (7) and $\Delta\lambda$ = 66 nm (**8**) in going from the non-polar toluene to the highly polar DMSO. Because of stronger mixing of dπ and π*

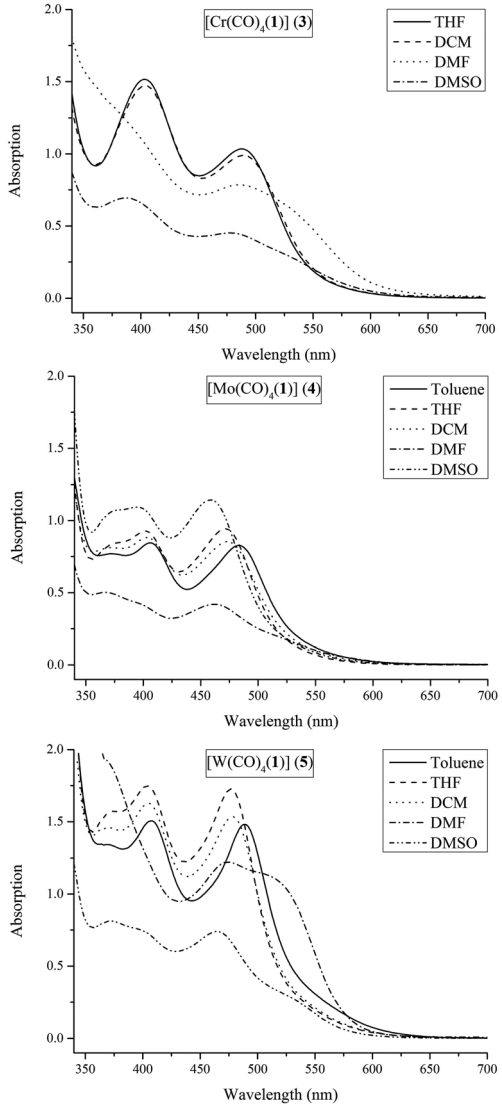

Fig. 10 Absorption spectra of the phosphinine-based complexes **3–5** measured in the solvent range from non-polar toluene to highly polar DMSO at T = 298 K, 1.25 × 10^{-4} M solutions.

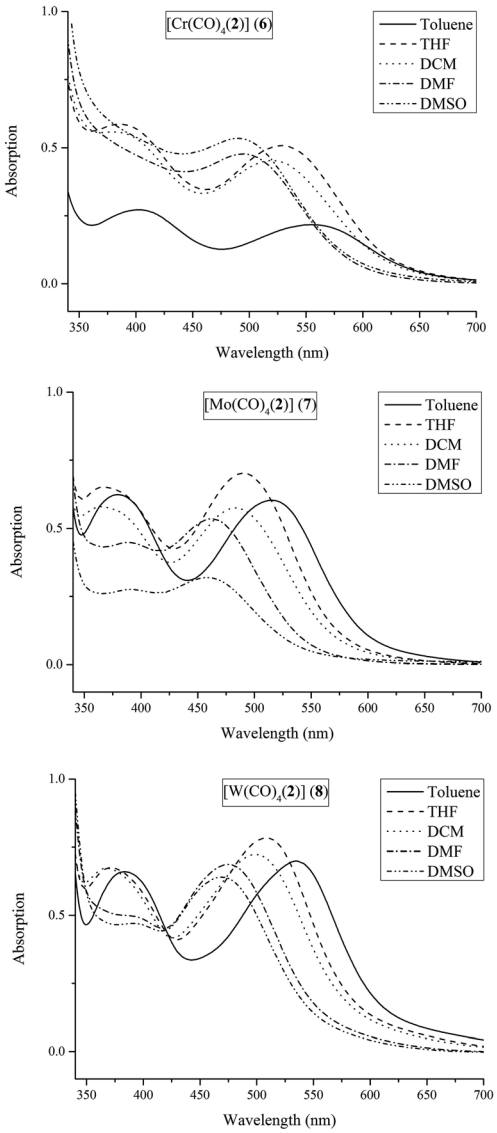

Fig. 11 Absorption spectra of the bipyridine-based complexes **6–8** measured in the solvent range from nonpolar toluene to highly polar DMSO at T = 298 K from 1.25 × 10^{-4} M solutions.

orbitals by π-backbonding the negative solvatochromism becomes smaller with increasing π-acceptor strength of the CO-ligand in $[M(CO_4)L_2]$ complexes due to a reduced charge transfer character in the MLCT transition. The here described results are thus perfectly in line with the IR-spectroscopic data, which point to a higher π-accepting character of the P,N-hybrid ligand **1**, in contrast to the bipyridine derivative **2**.

Cyclic voltammetry

We further investigated compounds **1** and **2** as well as the corresponding coordination compounds **3–8** by means of cyclic voltammetry and the results are shown in Fig. 12–14, as well as in Tables 6 and 7.

The phosphinine and its coordination compounds (**3–5**) have less negative reduction potentials compared to **2** and its coordination compounds (**6–8**). This is in excellent agreement with the relative energetic positions of the LUMOs. The LUMO of **1** is lower in energy than the LUMO of **2** and is thus easier to reduce than **2**. Moreover, both heterocyclic ligand systems show two reduction waves in the cyclic voltammogram.

The reduction processes of **1** are irreversible. The first reduction process of ligand **2** is also irreversible when measuring the full range from 1.8 to −3.0 V. However, when the measurement is stopped after the first reduction at −2.4 V, this process becomes reversible (see Table S1 and Fig. S1 in the ESI†). Furthermore, this process is a one electron reduction, which can be concluded from the differential pulse voltammetry measurement with ferrocene were the one electron oxidation peak of ferrocene and the first reduction peak of **2** have the same peak area (see Table S2 and Fig. S2 in the

Table 5 Absorption spectral data of **3–8** in solvents with increasing solvent polarity (λ_{max}/nm)[a]

	Toluene	THF	DCM	DMF	DMSO	Δ
[Cr(CO)$_4$(**1**)] (**3**)	—[b]	488	498	485	477	11
	—[b]	403	404	—[c]	387	16
[Mo(CO)$_4$(**1**)] (**4**)	483	470	473	462	459	24
	406	401	404	397	395	11
	373	378	364	364	376	—
[W(CO)$_4$(**1**)] (**5**)	489	479	478	473	464	25
	407	404	404	363	372	35
	369	376	370	—[c]	—[d]	—
[Cr(CO)$_4$(**2**)] (**6**)	554	528	520	494	490	64
	402	386	379	—[c]	—[d]	—
[Mo(CO)$_4$(**2**)] (**7**)	514	498	483	462	458	56
	380	364	364	389	391	—
[W(CO)$_4$(**2**)] (**8**)	535	508	498	474	469	66
	383	371	368	396	391	—

[a] At T = 289 K, 1.25 × 10^{-4} M solutions. [b] Insoluble. [c] Band coincides with solvent absorption. [d] Band coincides with other absorption.

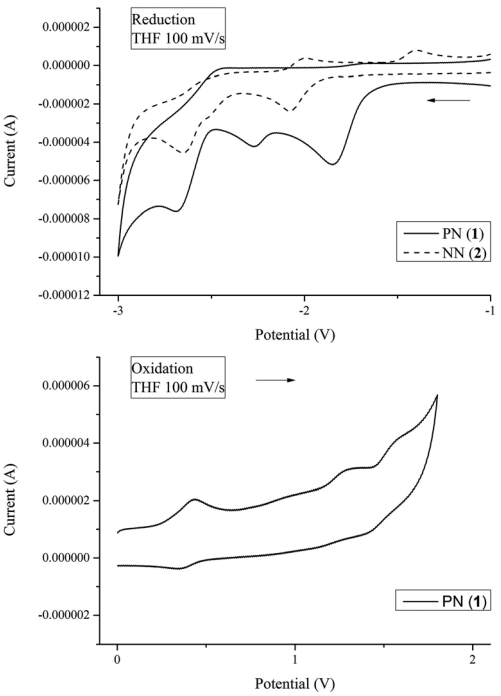

Fig. 12 Electrochemical spectra of ligand **1** and **2** determined by CV on a glassy carbon working electrode in 0.1 M nBu$_4$NPF$_6$ and 5 × 10^{-3} M THF solutions at T = 298 K.

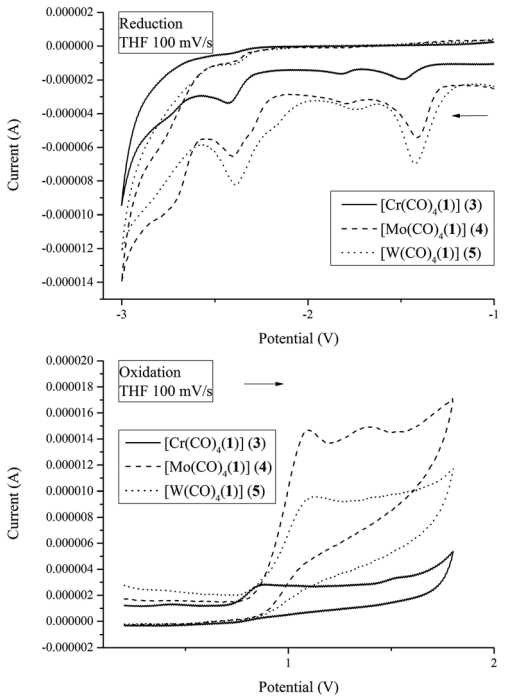

Fig. 13 Electrochemical spectra of phosphinine-based coordination compounds **3–5** determined by CV on a glassy carbon working electrode in 0.1 M nBu$_4$NPF$_6$ and 5 × 10^{-3} M THF solutions at T = 298 K.

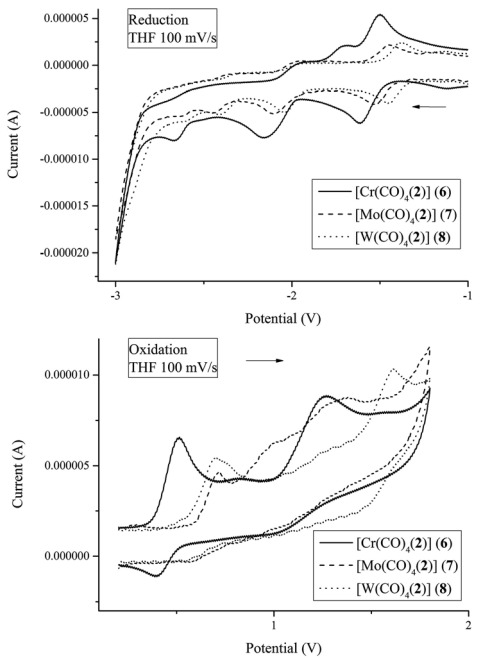

Fig. 14 Electrochemical spectra of bipyridine-based coordination compounds **6–8** determined by CV on a glassy carbon working electrode in 0.1 M nBu$_4$NPF$_6$ and 5 × 10^{-3} M THF solutions at T = 298 K.

ESI†). The second reduction process of **2** is also irreversible as observed for compound **1**. The coordination compounds **3–8** have three and four reduction waves. Coordination of ligand **1** and **2** to the metal center shifts the reduction potentials to more positive values, because the LUMO energy lowers upon coordination.[54,55] The shift of the first reduction towards positive potentials is essentially due to the fact that reduced forms of the ligand (L^- and L^{2-}) are more stabilized by ligation than the fully oxidized form of the ligand (L).[56,57] The shift is smaller for the phosphinine-based compounds **3–5** than for the pyridine-based compounds **6–8**. Again, we observed that the reduction waves of the phosphinine-based compounds **3–5**

Table 6 Electrochemical properties of ligand **1** and **2** and coordination compounds **3–8** determined by CV on a glassy carbon working electrode in 0.1 M nBu$_4$NPF$_6$ and 5 × 10^{-3} M THF solutions at T = 298 K[a,b]

	Reduction			
Compound	E_1	E_2	E_3	E_4
P,N (**1**)	−2.36[c]	−2.78[c]	−3.19[c]	—
[Cr(CO)$_4$(**1**)] (**3**)	−2.01[c]	−2.33[c,d]	−2.96[c]	−3.28[c,d]
[Mo(CO)$_4$(**1**)] (**4**)	−1.95[c]	−2.33[c,d]	−2.93[c]	−3.24[c,d]
[W(CO)$_4$(**1**)] (**5**)	−1.95[c]	−2.28[c,d]	−2.93[c]	—
N,N (**2**)	−2.61[c]	−3.18[c]	—	—
[Cr(CO)$_4$(**2**)] (**6**)	−2.10(105) *1.17*	−2.70[c]	—	−3.20[c]
[Mo(CO)$_4$(**2**)] (**7**)	−2.03(81) *1.62*	−2.63[c]	−2.98[c]	−3.17[c]
[W(CO)$_4$(**2**)] (**8**)	−1.96(71) *1.25*	−2.58[c]	−2.94[c]	−3.14[c]

[a] Values for (E_{pa} + E_{pc})/2 in V *vs.* Fc$^+$/Fc as internal standard, ΔE_{pc} in mV (in parentheses) I_{pc}/I_{pa} (in Italic) at a scan rate of 100 mV s^{-1}. [b] SCE reference electrode is used, Fc *vs.* SCE = 0.54(83)*0.81*. [c] Irreversible process, E_{pa} value in V reported. [d] Weak signal.

Table 7 Electrochemical properties of ligand **1** and **2** and coordination compounds **3–8** determined by CV on a glassy carbon working electrode in 0.1 M nBu$_4$NPF$_6$ and 5 × 10^{-3} M THF solutions at T = 298 K[a,b]

	Oxidation		
Compound	E_1	E_2	E_3
P,N (**1**)	−0.11[c]	0.72[c,d]	1.02[c,d]
[Cr(CO)$_4$(**1**)] (**3**)	—	0.33[c]	0.96[c]
[Mo(CO)$_4$(**1**)] (**4**)	—	0.53[c]	0.82[c]
[W(CO)$_4$(**1**)] (**5**)	—	0.55[c]	—
N,N (**2**)	—	—	—
[Cr(CO)$_4$(**2**)] (**6**)	−0.04[c]	—	0.69[c]
[Mo(CO)$_4$(**2**)] (**7**)	0.16[c]	0.43[c]	0.85[c]
[W(CO)$_4$(**2**)] (**8**)	0.17[c]	—	1.06[c]

[a] Values for (E_{pa} + E_{pc})/2 in V *vs.* Fc$^+$/Fc as internal standard, ΔE_{pc} in mV (in parentheses) I_{pc}/I_{pa} (in Italic) at a scan rate of 100 mV s^{-1}. [b] SCE reference electrode is used, Fc *vs.* SCE = 0.54(83)*0.81*. [c] Irreversible process, E_{pa} value in V reported. [d] Very weak signal which disappears after a few scans.

are all irreversible. The first reduction waves of **6–8** are irreversible when the spectra are recorded from 1.8 to −3.0 V. However, when measuring from 1.8 to −2.0 V, the first reduction process becomes reversible (see Tables S3–S5 and Fig. S3–S5 in the ESI†). This shows that the radical anions [M(CO)$_4$(**2**)]$^{\bullet-}$ are fairly stable.[58] The reversibility further indicates that the LUMO is a ligand-centered π* orbital. It was not possible to determine whether these reduction waves are one-electron reductions as differential pulse voltammetry measurements with equimolar ferrocene in the sample did not give equal integrals. Probably our coordination compounds behave differently than ferrocene does, making it impossible to compare them. The other reduction processes of **6–8** are irreversible.

It is known that the second reduction is also chemically irreversible for bpy or phenanthroline-based complexes, due to a fast dissociation of a CO ligand.[15] The third and fourth reductions belong to a complicated process which involves consumption of two and three electrons, respectively.[15] There is a clear and established order in that the heavier homologues display more positive reduction potentials.[54,55] In agreement with literature data the chromium complexes (**3** and **6**) have the most negative reduction potential followed by the molybdenum complexes (**4** and **7**) and the tungsten complexes (**5** and **8**) are most easy to reduce for both the phosphinine and bipyridine based complexes. Furthermore, the stabilization of reduced forms is evident from the equally shifted second reduction waves. The difference between reduction wave E_1 and E_2 is almost the same for all complexes and thus characteristic for the ligand system.[55]

In case of the bipyridine ligand **2**, no oxidation waves could be observed. The pyridyl-functionalized phosphinine **1**, however, shows three irreversible oxidation waves in the cyclic voltammogram. Nevertheless, the last two waves are very weak and disappears after a few scans. The electrochemical oxidations of all coordination compounds **3–8** are irreversible. This process corresponds to a loss of one electron from a metal-centered orbital. In fact, it is well-known that the +1 oxidation state of molybdenum and tungsten tetracarbonyl complexes is rather unstable.[15,54,59–61] From our measurements it appears that also the +1 oxidation states of the chromium complexes are unstable. This demonstrates the effect of the relatively high ligand basicity by destabilization of the highest occupied metal-based orbital. A high pK_a value of the ligand improves the complex stability of the coordination compounds because they have stronger σ-donor character. Although bipyridine derivative **2** does not show any oxidation waves, the bipyridine based coordination compounds (**6–8**) are easier to oxidize, indicating that ligand **2** has a higher pK_a value and is the stronger σ-donor compared to phosphinine-based ligand **1**, which is in agreement with the lower HOMO−2 level of **1**. Consequently, **1** is a weaker base than **2**, as also apparent from the molecular orbital scheme of phosphinines in comparison with pyridines. These results suggest that the reductions of the complexes **3–8** take place on the ligands, rather than on the metal center, which indicates a very small contribution of the metal d-orbitals to the LUMOs of the complexes.

Conclusions

The here presented results describe a detailed investigation of the structural and spectroscopic properties of 2-(2′-pyridyl)-4,6-diphenylphosphinine and its coordination compounds [M(CO)$_4$(P,N)] (M = Cr^0, Mo^0, W^0) in comparison to its structurally analogous bipyridine derivative 2-(2′-pyridyl)-4,6-diphenylpyridine. The air and moisture stable tetracarbonyl complexes containing the P,N-hybrid ligand can easily be obtained by ligand exchange reactions under thermal or photochemical conditions. In the latter case, a transient species is observed during the course of the reaction of [M(CO)$_6$] (M = Cr, W) with one equivalent of 2-(2′-pyridyl)-4,6-diphenylphosphinine,

revealing the formation of the intermediate species $[M(CO)_5(N,\eta^1\text{-}P)]$ prior to the formation of the final product. By means of competition experiments we could further show that 2-(2′-pyridyl)-4,6-diphenylphosphinine is the preferred chelate ligand for the coordination to an $M(CO)_4$ fragment, which is in line with the good π-accepting properties of this ligand. The structural analysis of the coordination compounds reveal significant differences between 2-(2′-pyridyl)-4,6-diphenylphosphinine and 2-(2′-pyridyl)-4,6-diphenylpyridine due to the larger size of the phosphorus atom compared to the nitrogen atom. The results of the IR-spectroscopic measurements, the presence of negative solvatochromism as well as the cyclic voltammetry investigations are in line with the higher π-accepting capacity of the phosphinine moiety compared to a pyridine system. These systematic investigations nicely demonstrate the differences between phosphorus and nitrogen containing heteroaromatic systems having otherwise identical structures. These informations are essential for the use of phosphinine-based coordination compounds in more applied research fields, such as catalysis and molecular materials.

Acknowledgements

C. M. and I. d. K. thank the Deutsche Forschungsgemeinschaft (DFG), the Netherlands Organization for Scientific Research (NWO-ECHO) and the Free University of Berlin for financial support. The X-ray diffractometer has been financed by NWO.

Notes and references

1 C. Kaes, A. Katz and M. W. Hosseini, *Chem. Rev.*, 2000, **100**, 3553.
2 O. Pàmies and J.-E. Bäckvall, *Chem. – Eur. J.*, 2001, **7**, 5052.
3 H. Yang, H. Gao and R. J. Angelici, *Organometallics*, 2000, **19**, 622.
4 M. S. Lowry and S. Bernhard, *Chem. – Eur. J.*, 2006, **12**, 7970.
5 A. J. Esswein and D. G. Nocera, *Chem. Rev.*, 2007, **107**, 4022.
6 D. A. Nicewicz and D. W. C. MacMillan, *Science*, 2008, **322**, 77.
7 K. Zeitler, *Angew. Chem., Int. Ed.*, 2009, **48**, 9785.
8 A. Savini, P. Belanzoni, G. Bellachioma, C. Zuccaccia, D. Zuccaccia and A. Macchioni, *Green Chem.*, 2011, **13**, 3360.
9 P. V. Pham, D. A. Nagib and D. W. C. MacMillan, *Angew. Chem., Int. Ed.*, 2011, **50**, 6119.
10 H. Ozawa and K. Sakai, *Chem. Commun.*, 2011, **47**, 2227.
11 T. J. Meyer, *Acc. Chem. Res.*, 1989, **22**, 163.
12 L. A. García-Esudero, D. Miguel and J. A. Turiel, *J. Organomet. Chem.*, 2006, **691**, 3434.
13 P. Datta, D. Sardar, A. Prasad Mukhopadhyay, E. López-Torres, C. J. Pastor and C. Sinha, *J. Organomet. Chem.*, 2011, **66**, 488.
14 A. Mentes, *Transition Met. Chem.*, 1999, **24**, 77.
15 A. Vlcek Jr., *Coord. Chem. Rev.*, 2002, **230**, 225.
16 Q. Ye, Q. Wu, H. Zhao, Y.-M. Song, X. Xue, R.-G. Xiong, S.-M. Pang and G.-H. Lee, *J. Organomet. Chem.*, 2005, **690**, 286.
17 R. W. Balk, T. Snoeck, D. J. Stufkens and A. Oskam, *Inorg. Chem.*, 1980, **19**, 3015.
18 P. Datta and C. Sinha, *Polyhedron*, 2007, **26**, 2433.
19 P. N. W. Baxter and J. A. Connor, *J. Organomet. Chem.*, 1995, **486**, 115.
20 D. J. Stufkens, *Coord. Chem. Rev.*, 1990, **104**, 39.
21 G. Märkl, *Angew. Chem., Int. Ed. Engl.*, 1966, **78**, 907.
22 L. Kollár and G. Keglevich, *Chem. Rev.*, 2010, **110**, 4257.
23 P. Le Floch, *Coord. Chem. Rev.*, 2006, **250**, 627.
24 N. Mezailles, F. Mathey and P. Le Floch, *Prog. Inorg. Chem.*, 2001, **49**, 455.
25 P. Le Floch and F. Mathey, *Coord. Chem. Rev.*, 1998, **179–180**, 771.
26 A. J. Ashe, *J. Am. Chem. Soc.*, 1971, **93**, 3293.
27 C. Müller, L. E. E. Broeckx, I. de Krom and J. J. M. Weemers, *Eur. J. Inorg. Chem.*, 2013, **2013**, 187.
28 C. Müller, J. A. W. Sklorz, I. de Krom, A. Loibl, M. Habicht, M. Bruce, G. Pfeifer and J. Wiecko, *Chem. Lett.*, 2014, **43**, 1390.
29 J. M. Alcaraz, A. Breque and F. Mathey, *Tetrahedron Lett.*, 1982, **23**, 1565.
30 P. Le Floch, D. Carmichael, L. Ricard and F. Mathey, *J. Am. Chem. Soc.*, 1993, **115**, 10665.
31 I. de Krom, L. E. E. Broeckx, M. Lutz and C. Müller, *Chem. – Eur. J.*, 2012, **19**, 3676.
32 A. Campos Carrasco, E. A. Pidko, A. M. Masdeu-Bultó, M. Lutz, A. L. Spek, D. Vogt and C. Müller, *New J. Chem.*, 2010, **34**, 1547.
33 I. de Krom, E. A. Pidko, M. Lutz and C. Müller, *Chem. – Eur. J.*, 2013, **19**, 7523.
34 C. Müller and D. Vogt, *Dalton Trans.*, 2007, 5505.
35 C. Müller and D. Vogt, in *Catalysis and Material Science Applications*, ed. M. Peruzzini and L. Gonsalvi, Springer, 2011, ch. 6, vol. 36.
36 P. D. Burrow, A. J. Ashe, D. J. Bellville and K. D. Jordan, *J. Am. Chem. Soc.*, 1982, **104**, 425.
37 L. Nyulászi, *Chem. Rev.*, 2001, **101**, 1229.
38 L. Nyulászi and T. Veszpremi, *J. Phys. Chem.*, 1996, **100**, 6456.
39 A. Modelli, B. Hajgato, J. F. Nixon and L. Nyulászi, *J. Phys. Chem. A*, 2004, **108**, 7440.
40 J. Waluk, H. P. Klein, A. J. Ashe and J. Michl, *Organometallics*, 1989, **8**, 2804.
41 A. Campos Carrasco, L. E. E. Broeckx, J. J. M. Weemers, E. A. Pidko, M. Lutz, A. M. Masdeu-Bultó, D. Vogt and C. Müller, *Chem. – Eur. J.*, 2011, **17**, 2510.
42 C. Müller and D. Vogt, *C. R. Chim.*, 2010, **13**, 1127.
43 L. E. E. Broeckx, M. Lutz, D. Vogt and C. Müller, *Chem. Commun.*, 2011, **47**, 2003.
44 A. Brèque, C. C. Santini, F. Mathey, J. Fischer and A. Mitschler, *Inorg. Chem.*, 1984, **23**, 3463.

45 J. Deberitz and H. Nöth, *J. Organomet. Chem.*, 1973, **49**, 453.
46 E. Moser, E. O. Fischer, W. Bathelt, W. Gretner, L. Knauss and E. Louis, *J. Organomet. Chem.*, 1969, **19**, 377.
47 B. Schmid, L. M. Venanzi, T. Gerfin, V. Gramlich and F. Mathey, *Inorg. Chem.*, 1992, **31**, 5117.
48 C. Müller, M. Lutz, A. L. Spek and D. Vogt, *J. Chem. Crystallogr.*, 2006, **36**, 869.
49 M. Doux, L. Ricard, F. Mathey, P. Le Floch and N. Mézailles, *Eur. J. Inorg. Chem.*, 2003, 687.
50 P. Le Floch, D. Carmichael, L. Ricard and F. Mathey, *J. Am. Soc. Chem.*, 1991, **113**, 667.
51 R. W. Balk, D. J. Stufkens and A. Oskam, *Inorg. Chim. Acta*, 1979, **34**, 267.
52 P. C. Servaas, H. K. van Dijk, T. L. Snoeck, J. Stufkens and A. Oskam, *Inorg. Chem.*, 1985, **24**, 4494.
53 R. B. Ali, J. Burgess, M. Kotowski and R. van Eldik, *Transition Met. Chem.*, 1987, **12**, 230.
54 S. Ernst and W. Kaim, *J. Am. Chem. Soc.*, 1986, **108**, 3578.
55 W. Kaim and S. Kohlmann, *Inorg. Chem.*, 1987, **26**, 68.
56 D. Miholová, B. Gaš, S. Záliš, J. Klíma and A. A. Vlcek, *J. Organomet. Chem.*, 1987, **330**, 75.
57 A. A. Vlcek, *Coord. Chem. Rev.*, 1982, **43**, 39.
58 I. R. Farrell, F. Hartl, S. Záliš, T. Mahabiersing and A. A. Vlcek, *J. Am. Chem. Soc., Dalton Trans.*, 2000, 4323.
59 R. J. Crutchley and A. B. P. Lever, *Inorg. Chem.*, 1982, **21**, 2276.
60 H. T. Dieck and E. Kühl, *Z. Naturforsch. B: Anorg. Chem. Org. Chem.*, 1982, **37**, 324.
61 S. Ernst and W. Kaim, *Inorg. Chim. Acta*, 1986, **114**, 123.